Four-Way Lossless Outphasing and Power Combining with Hybrid Microstrip/Discrete Combiner for Microwave Power Amplification

Taylor W. Barton, Joel L. Dawson, and David J. Perreault

Massachusetts Institute of Technology, Cambridge, MA 02139

Abstract— **This work demonstrates a four-way outphasing and power combining system for microwave power amplification using a novel power combining network. The ideally lossles combining network is implemented using a combination of microstrip transmission-line sections with discrete shunt elements. We present the derivation of the power combining network topology as well as practical implementation details.**

The new power combining network is demonstrated in a 50-W, 2.14-GHz power amplifier system using load modulation of switching GaN PAs through outphasing for output power control. The system has a peak CW drain efficiency of 59.5% and drain efficiency above 45% over a 8.17-dB outphasing output power range. In modulated tests with a signal bandwidth of 3.84 MHz, the system demonstrates 52% average drain efficiency for a 3.9-dB peak to average power ratio (PAPR) signal, and 38% drain efficiency for a W-CDMA signal with 9.6 PAPR.

Index Terms— **base stations, outphasing, LINC, Chireix, power amplifiers.**

I. INTRODUCTION

A major challenge in microwave power amplifier (PA) design for communications is the linearity requirements resulting from high peak-to-average power ratios (PAPRs) in transmitted signals. For efficient amplification of modulated signals, this linearity must be realized simultaneously with high efficiency over a wide range of output powers.

Switching PAs implemented using GaN devices are highly attractive for efficient power amplification in high frequency, high power applications. An overall linear response can be achieved using by combining the outputs of multiple of these nonlinear switching PAs. Chireix outphasing is an example of this technique, using a lossless, non-isolating power combining network such that the real part of the load seen by each PA depends on the relative (outphasing) angle of the PA inputs [1], [2]. A drawback of the Chireix technique is that the imaginary part of the PA loading also varies significantly with outphasing angle.

A four-way outphasing and power combining system was recently proposed that provides nearly resistive load modulation of PAs operating in switched mode [3], [4]. The combiner utilized in [3], [4] and tested at HF frequencies uses discrete (lumped) elements connected in a tree structure. In [5] it is shown that this technique can be extended to microwave frequencies by careful tuning and accounting for the electrical lengths of components and interconnects. Although the design in [5] was successful, the approach relies on significant hand-tuning of discrete component values in order to synthesize the power combining network. It would be desirable to gain the benefit of this multi-way outphasing approach in a manner that is more suitable for use at microwave frequencies.
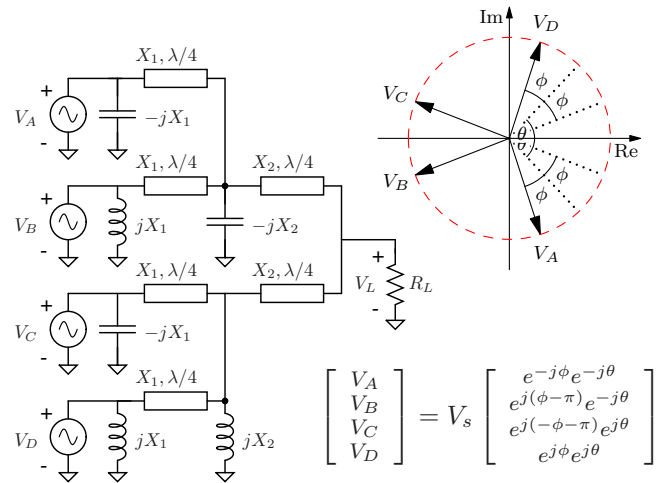

Fig. 1. Four-way power combiner implementation using shunt reactive components and microstrip transmission-line sections, and phasor relationship of the four PA input voltages. The PAs are represented as ideal voltage sources.

In this work we present a new microwave-oriented implementation of the four-way outphasing system. By properly incorporating transmission lines, we are able to realize a combiner that only uses discrete elements to provide shunt reactances. Limiting the use of discrete components in this way avoids the necessity of fully accounting for the non-ideal behaviors of these elements at microwave frequencies. Such nonidealities include non-zero electrical length and parasitic capacitance to ground. These factors can readily be absorbed into the reactance value when the element is used in a shunt connection to ground. Moreover, this implementation inherently provides for the necessary physical spacing of power amplifiers in a practical system.

II. POWER COMBINING NETWORK

A. Theoretical Development

The proposed four-way outphasing and power combining system is shown in Fig. 1, with the PAs represented as ideal voltage sources. This network can be related to the four-way power combining network proposed in [3] by applying the transformation indicated in Fig. 2. The two networks shown have identical input impedances, $Z_{\text{in},1} = Z_{\text{in},2}$, and equal magnitudes for the terminal voltages, $|v_{a1}| = |v_{a2}| = |v_{b1}| = |v_{b2}|$. The phases of v_{a1} and v_{a2} are equal, but $\angle v_{b1}$ and $\angle v_{b2}$ differ by $180°$. Applying these port relationships to the network in [3], it is found that when the four inputs to the power combining network are driven with the relationship
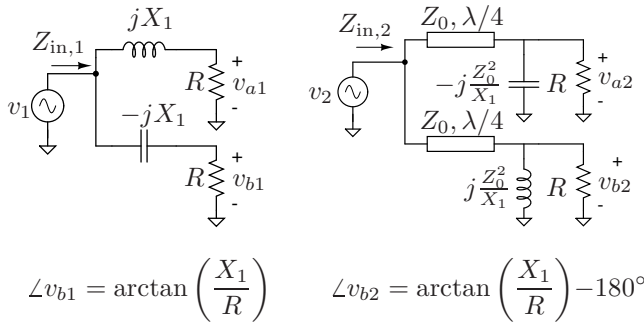
Fig. 2. Network transformation between two variations of the single-stage resistance compression network. Input impedances and terminal voltage amplitudes are identical.
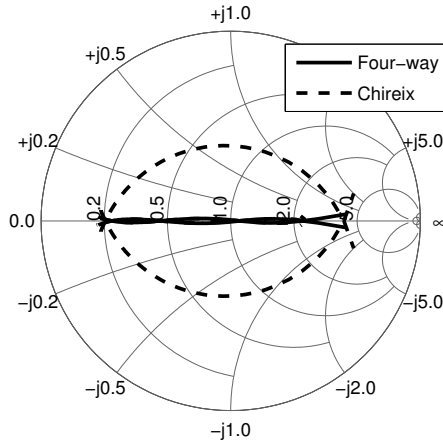

Fig. 3. Smith chart showing theoretical load impedances for the four PAs in this architecture when $X_1 = 35.6 \ \Omega$, $X_2 = 48.78 \ \Omega$, and $R_L = 50 \ \Omega$ (solid lines). For comparison, PA loading is also shown for a Chireix combiner with $R = 19.4 \ \Omega$ and $X = 45 \ \Omega$ (dashed line).

given in Fig. 1, the port input impedances will be identical to those found in [3]. Therefore the outphasing control law (1) may be used [3]. This phase relationship is shown graphically in Fig. 1.

$$\theta = \cos^{-1}\left(\sqrt{\frac{P_n}{4} + \frac{1}{4P_n}\left(\frac{X_1}{R_L}\right)^2}\right),$$

$$\phi = \tan^{-1}\left(\frac{X_1}{R_L P_n}\right) \tag{1}$$

It can be shown that the apparent port admittances at the four inputs, when all sources are active and operating with the relationship in Fig. 1 will be nearly resistive over a wide dynamic range. For the combiner reactance values used in this work, namely $X_1 = 35.6 \ \Omega$, $X_2 = 48.78 \ \Omega$, and $R_L = 50 \ \Omega$, the phase of the load admittance is calculated to be under $2°$ over a 10-dB range of output power. This loading is shown in Fig. 3, along with the PA loading for a Chireix combiner with similar output power range, values $R = 19.4 \ \Omega$, $X = 45 \ \Omega$.

B. Prototype Implementation

The combiner layout for a 2.14-GHz prototype system, implemented on a 30-mil thick Rogers 4350B substrate, is
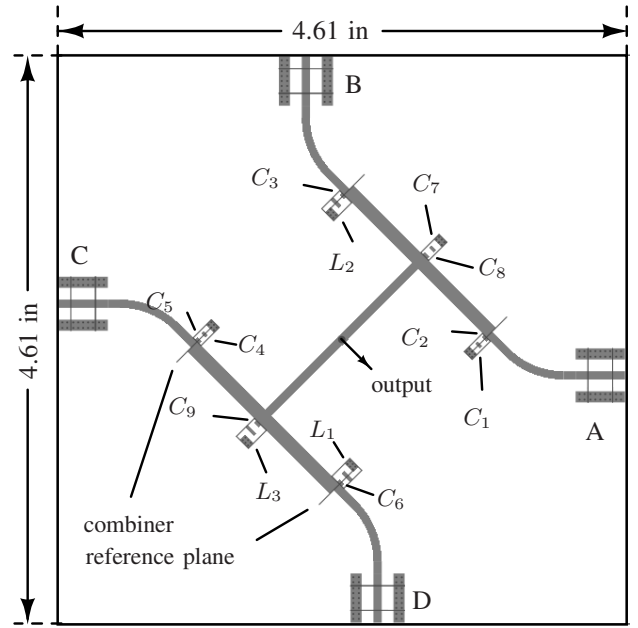

Fig. 4. Annotated 2.14-GHz combiner layout showing component labels. Combiner input reference planes are indicated in silkscreen. The vertical SMA output connector is mounted on the reverse side. Outer dimensions are 4.61"× 4.61".

shown in Fig. 4. Shunt reactive elements are implemented using series-connected discrete components, either C-C or L-C, to allow for tuning of the net reactance to ground at each node. The inductive branches in particular require an L-C series combination due to the relatively widely-spaced values available in the CoilCraft Micro Spring air core inductors used. It is important to note that this combiner topology is less sensitive to component electrical length than the series-element topology in [5], as discrete components are used only in shunt connections. The electrical length of the C-C or L-C connection plus solder pad shunt capacitance can be absorbed into the reactance. Component values are selected through an iterative trimming process to address this and other nonidealities of the reactive elements.

Component values are selected by characterizing the network in reverse as a power splitter, i.e. by driving the output port and measuring the magnitude and phase of the forward voltage gain to the four 50-Ω terminated input ports. The $\pm jX_2$ elements are populated first and adjusted until the magnitude of the forward voltage gain from the output to ports A and C (or B and D) are equal and the phases have the expected relationship. Then the relationships between ports A and B, and between C and D, are set by populating the $\pm jX_1$ components. Table I summarizes the component values used in this work, resulting in the forward voltage gains in Table II when all ports are terminated with 50 Ω.

The reference planes defining the inputs to the power combining network are indicated in Fig. 4. The length of the connection between these reference planes and the reference planes of the PAs must be chosen to provide a net quarter-

Component	Value	Mfr. Part #	Mfr.
C_8, C_9	0.2 pF ||	600F 0R2BT	
	1.2 pF	600F 1R2BT	American
C_3, C_6	1.5 pF	600F 1R5BT	Technical
C_7	2.0 pF	600F 2R0TC	Ceramics
C_1, C_4	2.4 pF	600F 2R4BT	Corp.
C_2, C_5	2.7 pF	600F 2R7BT	
L_1-L_3	3.85 nH	0906-4GLB	CoilCraft

TABLE II

MEASURED AND IDEAL PORT RELATIONSHIPS WHEN OUTPUT IS DRIVEN
AND ALL PORTS ARE TERMINATED WITH 50 Ω.

Port	Measured Ampl.	Measured Phase	Ideal Phase
A	1.08	95	88
B	0.97	-164	-163
C	0.94	163	163
D	1.01	-96	-88

Fig. 6. Measured drain efficiency and output power when input drive is held constant at maximum amplitude: (dashed) - calculated from individual PA measurements and assuming ideal, lossless power combining; (solid) - system performance using outphasing for output power control.

or half-wave electrical length so that the real impedances at the combiner inputs appear as real loads to the PAs. In this implementation, we included additional SMA adapters between the two PCBs to get the correct total electrical length. The combiner insertion loss including connectors is measured to be 0.41 dB by measuring the total power transmission to the four input ports when the output is driven with 20 dBm. It would be straightforward to partially reduce this loss by shortening the on-combiner 50-Ω traces to shorten the interconnection between boards by a quarter wavelength.

III. EXPERIMENTAL RESULTS

A photograph of the RF power stage of the experimental system is shown in Fig. 5. The phase-modulated PA inputs are implemented using Analog Devices AD9779A 16-bit DAC evaluation boards with upconverting mixers. An FPGA provides an interface b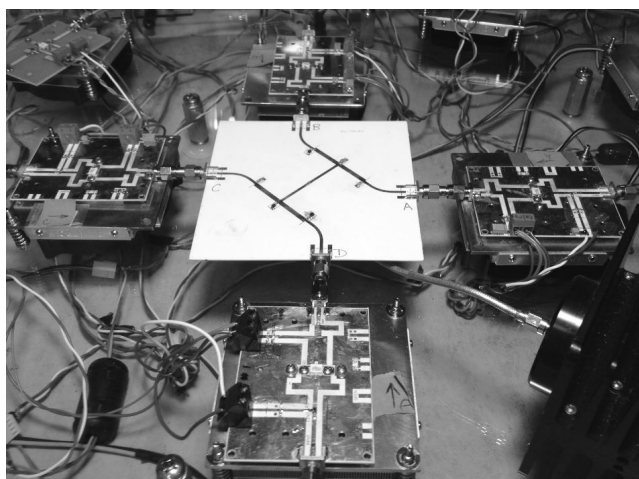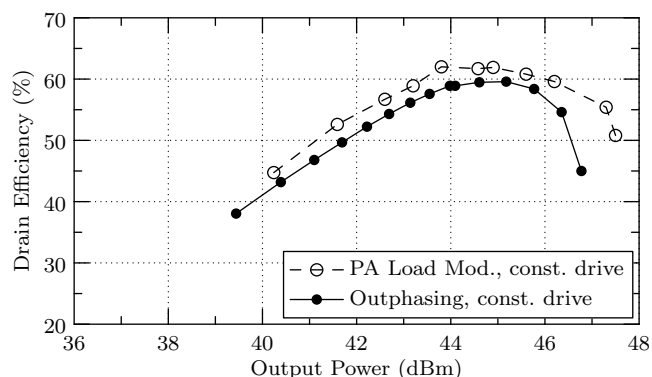etween the computer performing signal separation and the phase modulator PCBs. The power stage includes four Inverse Class F PAs following the design in [6] and operated with a gate bias of -3.4 V and a supply voltage of 20 V.

The Inverse Class F PAs are individually characterized under load modulation in order to find a theoretical maximum performance of the outphasing system. The PA output powers and drain efficiencies are measured when each PA is driven with the maximum drive amplitude and loaded with a range of real impedances corresponding to those in the combiner system. The output powers are then summed assuming zero combining loss, and the drain efficiencies are averaged. The resulting curve (see dashed curve in Fig. 6) represents the theoretical maximum performance of the outphasing power combiner system using these PAs.

A. System CW Measurements

The outphasing system measurements in Fig. 6 are performed by varying the relative phase of the four CW PA inputs based on the outphasing control law in (1). As for the inverse class F PA characterization, this measurement is performed with a constant-amplitude input to the switching PAs. The close match between these outphasing results and the theoretical maximum performance indicates that the combiner is functioning as expected.

In practice, it is preferable to reduce the drive amplitude at lower system output powers in order to avoid overdriving the switching PAs. Backing off the amplitude drive in this way avoids efficiency loss due to overdriving and improves the system power-added efficiency. Using the piecewise linear backoff control law indicated in Fig. 7 extends the outphasing operation to a 9.46-dB range, with the system drain efficiency above 45% for the upper 8.17 dB of this range. Below the outphasing control range, the outphasing angle is held constant and drive amplitude control alone is used to modulate the output power. This outphasing plus drive modulation control method is used for the modulated measurements below.

Fig. 5. Photograph of the RF power stage of the outphasing PA system.
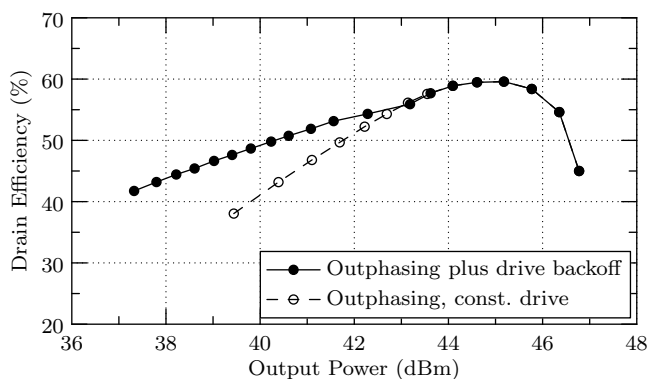
(a)
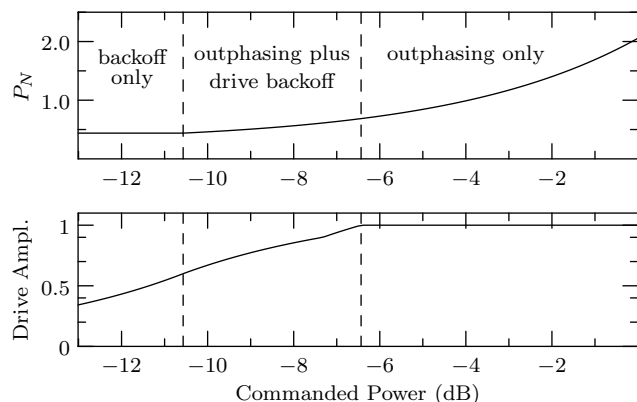
(b)

Fig. 7. Outphasing plus drive amplitude backoff, (a) - outphasing results with (solid) and without (dashed) input drive backoff, and (b) - control law for outphasing command P_N and drive amplitude. Combining drive amplitude control with outphasing prevents overdriving of the switched-mode PAs.

B. Modulated Performance

Table III contains a summary of the system performance demonstrating W-CDMA modulation. Results for both UE (3.9 dB) and BTS (9.6 dB) signals are shown, using a memoryless lookup-table for digital predistortion. Also shown in this table is a comparison of power amplifier efficacy, defined as the ratio of average modulated drain efficiency to peak CW efficiency. The efficacy of this work is comparable to the state of the art. Compared to the lumped-element version of this technique [5], this implementation has improved efficacy due to its wider outphasing control range.

TABLE III
COMPARISON TO OTHER WORKS: WCDMA PERFORMANCE

Ref.	Arch	Carrier (MHz)	PAPR (dB)	P_{out} (dBm)	Drain Eff.	Efficacy
[7]	Chireix	2140	9.6	39.5	50.5%	65%
[6]	Doherty	2140	6.5	43	61%	79%
[8]	Doherty	2600	7	57.3	48%	78%
[5]	4-way Discrete	2140	3.47	42	57%	80%
This Work	4-way Hybrid	2140	3.9	41.9	52%	87%
			9.6	35.9	38%	64%

IV. CONCLUSION

The new four-way outphasing system demonstrated in this work has been designed specifically for microwave frequencies. We use transmission lines to adapt the network described in [3] into one that uses lumped elements only in shunt connections rather than in the power path. This approach has greater ease of fabrication than that in [5], as well as greater potential for extension to higher frequencies. Experimental results at 2.14-GHz demonstrate the effectiveness of the approach.

REFERENCES

[1] I. Hakala, D. Choi, L. Gharavi, N. Kajakine, J. Koskela, and R. Kaunisto, "A 2.14-GHz Chireix outphasing transmitter," *IEEE Trans. Microw. Theory and Techn.*, vol. 53, no. 6, pp. 2129–2138, June 2005.

[2] N. Singhal, H. Zhang, and S. Pamarti, "A zero-voltage-switching contour-based outphasing power amplifier," *IEEE Trans. Microw. Theory and Techn.*, vol. 60, no. 6, pp. 1896–1906, June 2012.

[3] D. Perreault, "A new power combining and outphasing modulation system for high-efficiency power amplification," *IEEE Trans. Circuits Syst. I, Reg. Papers*, vol. 58, no. 8, pp. 1713 –1726, Feb. 2011.

[4] A. Jurkov, L. Roslaniec, and D. Perreault, "Lossless multi-way power combining and outphasing for high-frequency resonant inverters," in *2012 Int'l Power Electronics and Motion Control Conf.*, June 2012, pp. 910–917.

[5] T. W. Barton, J. L. Dawson, and D. J. Perreault, "Experimental validation of a four-way outphasing combiner for microwave power amplification," *IEEE Micro. Wireless Compon. Lett.*, vol. 23, no. 1, pp. 28–30, Jan. 2013.

[6] A. Grebennikov, "A high-efficiency 100-W four-stage Doherty GaN HEMT power amplifier module for WCDMA systems," in *IEEE 2011 Int. Microwave Symp.*, June 2011, pp. 1 –4.

[7] J. Qureshi and et al, "A 90-W peak power GaN outphasing amplifier with optimum input signal conditioning," *IEEE Trans. Microw. Theory Techn.*, vol. 57, no. 8, pp. 1925–1935, Aug. 2009.

[8] H. Deguchi and et al, "A 2.6GHz band 537W peak power GaN HEMT asymmetric Doherty amplifier with 48% drain efficiency at 7dB," in *IEEE 2012 Int. Mircowave Symp.*, June 2012, pp. 1 –3.